

RESEARCH

Open Access



# RIPK1 inhibition mitigates neuroinflammation and rescues depressive-like behaviors in a mouse model of LPS-induced depression

Qichao Gong<sup>1</sup>, Tahir Ali<sup>1</sup>, Yue Hu<sup>1</sup>, Ruyan Gao<sup>1</sup>, Shengnan Mou<sup>1</sup>, Yanhua Luo<sup>1</sup>, Canyu Yang<sup>2</sup>, Axiang Li<sup>2</sup>, Tao Li<sup>2</sup>, Liang Liang Hao<sup>3</sup>, Liufang He<sup>4\*</sup>, Xiaoming Yu<sup>5\*</sup> and Shupeng Li<sup>1,6\*</sup>

## Abstract

**Background** Depression is often linked to inflammation in the brain. Researchers have been exploring ways to reduce this inflammation to improve depression symptoms. One potential target is a protein called RIPK1, which is known to contribute to brain inflammation. However, it's unclear how RIPK1 influences depression. Our study aims to determine whether RIPK1 inhibition could alleviate neuroinflammation-associated depression and elucidate its underlying mechanisms.

**Methods** To investigate our research objectives, we established a neuroinflammation mouse model by administering LPS. Behavioral and biochemical assessments were conducted on these mice. The findings were subsequently validated through in vitro experiments.

**Results** Using LPS-induced depression models, we investigated RIPK1's role, observing depressive-like behaviors accompanied by elevated cytokines, IBA-1, GFAP levels, and increased inflammatory signaling molecules and NO/H<sub>2</sub>O<sub>2</sub>. Remarkably, Necrostatin (Nec-1 S), a RIPK1 inhibitor, mitigated these changes. We further found altered expression and phosphorylation of eIF4E, PI3K/AKT/mTOR, and synaptic proteins in hippocampal tissues, BV2, and N2a cells post-LPS treatment, which Nec-1 S also ameliorated. Importantly, eIF4E inhibition reversed some of the beneficial effects of Nec-1 S, suggesting a complex interaction between RIPK1 and eIF4E in LPS-induced neuroinflammation. Moreover, citronellol, a RIPK1 agonist, significantly altered eIF4E phosphorylation, indicating RIPK1's potential upstream regulatory role in eIF4E and its contribution to neuroinflammation-associated depression.

**Conclusion** These findings propose RIPK1 as a pivotal mediator in regulating neuroinflammation and neural plasticity, highlighting its significance as a potential therapeutic target for depression.

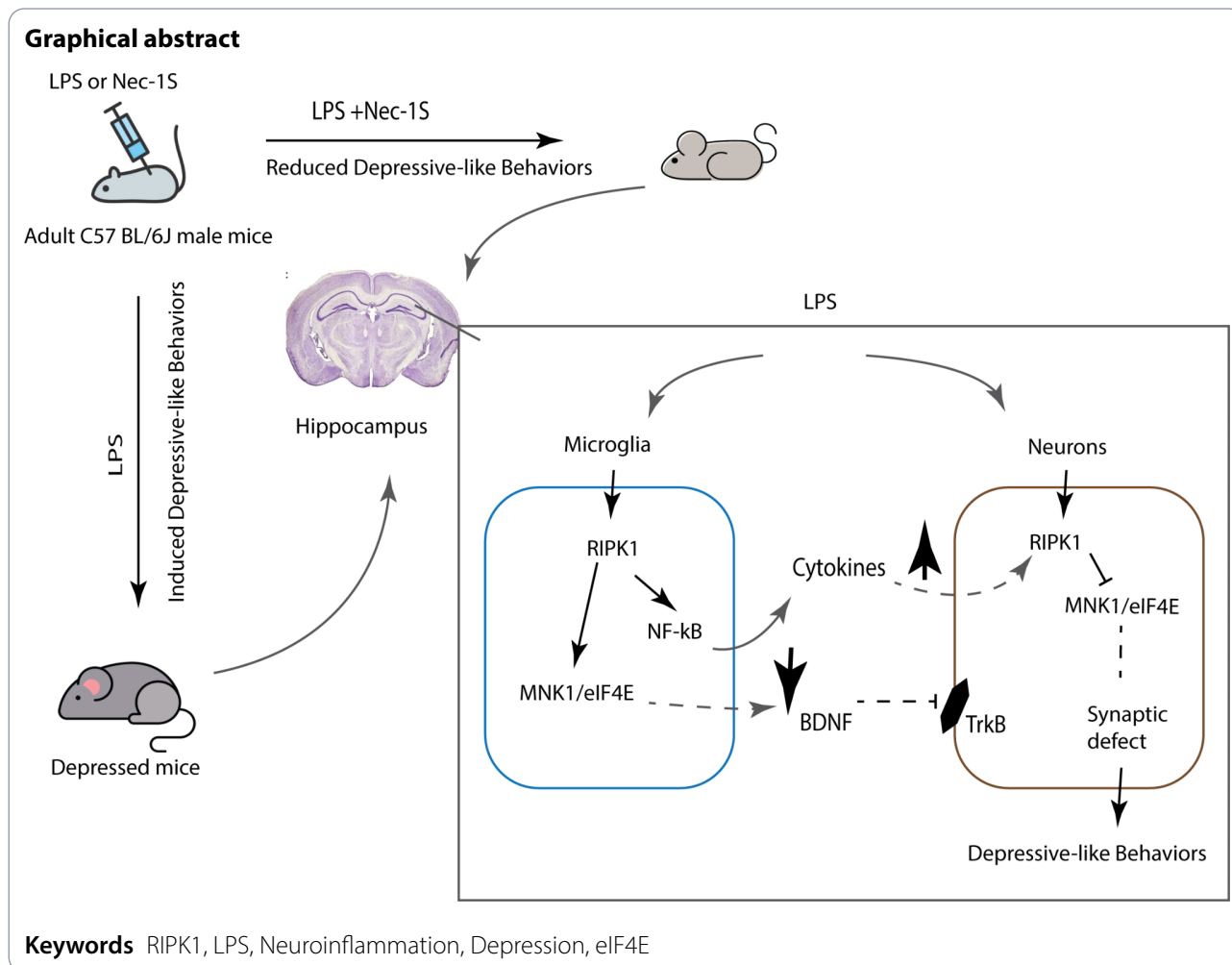
\*Correspondence:

Liufang He  
heliufang6022@163.com  
Xiaoming Yu  
yuxiaoming1927@email.sdu.edu.cn  
Shupeng Li  
lisp@pku.edu.cn

Full list of author information is available at the end of the article



© The Author(s) 2024. **Open Access** This article is licensed under a Creative Commons Attribution-NonCommercial-NoDerivatives 4.0 International License, which permits any non-commercial use, sharing, distribution and reproduction in any medium or format, as long as you give appropriate credit to the original author(s) and the source, provide a link to the Creative Commons licence, and indicate if you modified the licensed material. You do not have permission under this licence to share adapted material derived from this article or parts of it. The images or other third party material in this article are included in the article's Creative Commons licence, unless indicated otherwise in a credit line to the material. If material is not included in the article's Creative Commons licence and your intended use is not permitted by statutory regulation or exceeds the permitted use, you will need to obtain permission directly from the copyright holder. To view a copy of this licence, visit <http://creativecommons.org/licenses/by-nc-nd/4.0/>.



## Introduction

Major depressive disorder (MDD) is a complex mental health condition characterized by persistent sadness, loss of interest, and other symptoms. It's associated with changes in brain function, including alterations in mood, communication between nerve cells (synaptic defects), and overall brain structures [1–5]. Mounting evidence suggests that inflammation plays a significant role in depression. Studies have found increased levels of inflammatory markers, such as interleukin-6 (IL-6), in the blood of people with depression [6, 7]. Additionally, brain tissue from individuals with depression often shows increased levels of inflammatory molecules, including tumor necrosis factor- $\alpha$  (TNF- $\alpha$ ) [8]. This inflammation can trigger a chain reaction in the brain, leading to damage to brain cells, impaired communication between neurons, and changes in brain structure [4, 5, 9–11]. While we know inflammation is involved, more research is needed to understand how it contributes to depression fully.

Receptor Interacting Serine/Threonine Kinase 1 (RIPK1) is a 76-kDa protein with a death domain at

the carboxy-terminal (C-terminal), a kinase domain at an amino-terminal (N-terminal), and an intermediate domain with a receptor-interacting protein homotypic interacting motif (RHIM). It is a crucial regulator of cell death pathways and is essential for mediating pro-survival nuclear factor kappa B subunit (NF- $\kappa$ B) signaling. Besides, it also participates in the signaling pathways of various cytokines, including TNF- $\alpha$  and interleukins, which are critical for immune response and inflammation [12, 13]. Moreover, RIPK1 may cause detrimental neuroinflammatory environments in neurological diseases [14, 15]. However, it is unclear whether differential signals exist downstream of distinct RIPK1-activating stimuli and how they contribute to neuroinflammation during depressive disorders. Our data reveal that lipopolysaccharides (LPS) activates RIPK1 concurrent with neuroinflammation. Activated RIPK1 dysregulates downstream phosphatidylinositol 3-kinase (PI3K) and, most importantly, Eukaryotic Initiation Factor 4E (eIF4E) signaling. PI3K and serine-threonine protein kinase (Akt) signaling cascade is a highly conserved intracellular

pathway involved in the phospholipid and protein phosphorylation of various downstream targets in the cellular responses [16, 17]. In addition, RIPK1 enhances the transcription of inflammatory cytokines through activation of the eIF4E-mediated cap-dependent translation initiation process [18, 19]. Moreover, this multifaceted signaling pathway regulates proinflammatory cytokine expression and potentially modulates neurotransmitter activity [16]. Downstream of PI3K/Akt, inhibition of eIF4E, a key protein synthesis regulator implicated in neuropsychiatric disorders through its association with brain-derived neurotrophic factors (BDNF) and Glutamate receptor 1 (GluR1) dysregulation [20, 21], exacerbates LPS-induced neuroinflammation and depressive-like behaviors alongside synaptic impairments. These findings highlight the critical role of RIPK1/eIF4E in mediating LPS-induced neuroinflammation and depression.

## Methods

### Animals

Adult C57 BL/6J male mice weighing 20–22 g (age 6–8 weeks) were purchased from Guangdong Medical Laboratory Animal Center, China. The experimental animals were housed ( $n=4/\text{cage}$ ) with free food and tap water access at the Laboratory Animal Research Center, Peking University Shenzhen Graduate School, under a 12 h light/12 h dark cycle at 18–22 °C. All experimental procedures were performed according to the protocols approved by the Peking University Shenzhen Graduate School Institutional Animal Care and Use Committee. The experimental procedures were designed to minimize animal suffering.

### Experimental design for drug treatment

The study was conducted in two experiments.

In the first experiment, animals were divided into three groups (10–12 mice/group): normal saline-treated (NC), LPS (1 mg/kg, once a day, i.p.) treated, and LPS+Nec-1 S (10 mg/kg, once a day, i.p.). (Fig. 1A).

In the second experiment, mice were treated with eFT508 in the presence of LPS and Nec-1 S. The animal groups were LPS-treated, LPS+Nec-1 S, and LPS+Nec-1 S+eFT508 (5 mg/kg, once daily, i.p.). (Fig. 2A).

After 48 h of the last LPS injection, mice were sacrificed after behavior analysis. Brain tissues were collected and stored at freezing temperatures (-80 °C) until further investigation.

The Nec-1 S (CAS No.: 852391-15-2) used in this study was purchased from Guangzhou Isunpharm. The LPS was purchased from Sigma-Aldrich. The eFT508 (CAS No.: 1849590-01-7) used in this study was purchased from Shanghai Send Pharm, prepared as described for in vivo dosing, and diluted in 0.9% saline. The Citronellol

(CAS No.: 7540-51-4) was purchased from Shanghai Haohong Scientific Co., Ltd., and the Wortmannin (CAS No.: 19545-26-7) was purchased from Henan Alfa Chemical Co., Ltd.

LPS was dissolved in saline for animal treatments and in phosphate-buffered saline (PBS) for cell treatments. Nec-1 S, eFT508, Wortmannin, and Citronellol were initially dissolved in dimethyl sulfoxide (DMSO) and subsequently diluted in saline for animal treatments or culture medium for cell treatments.

For in vitro studies, LPS was dissolved in PBS and added to the culture medium at a final concentration of 100 ng/mL for 4 h. Nec-1 S was dissolved in DMSO and added to the culture medium at final concentrations ranging from 1 to 20  $\mu\text{M}$  for 12 h.

### Behavior analysis

#### Open field test (OFT)

OFT was performed following the previously developed protocols [22]. Briefly, mice were adapted to the experimental room for one hour and placed in the 45×45×30 cm chamber. A total of 5 min of video was recorded to observe the mice's locomotor activity. The total distance covered by mice was measured, analyzed, and expressed in meters.

#### Sucrose preference test (SPT)

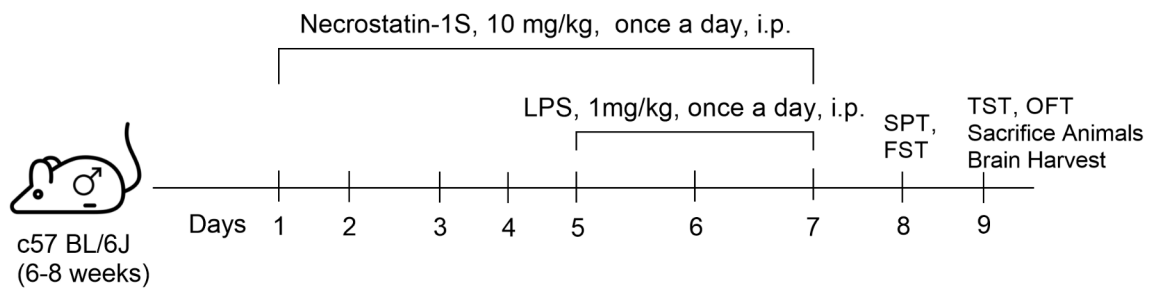
A sucrose preference test was performed while using a two-bottle free-choice paradigm. To assess the individual sucrose intake, mice were deprived of water and food for one night on the last day of the LPS administration. Each mouse had free access to two sucrose and water bottles the next day. The position of water and sucrose-containing bottles was changed after 2.5 h. Finally, the volume of consumed water and sucrose solution was recorded and calculated by the following formula:

$$SPT = \frac{\text{Sucrose consumption}}{\text{water and Sucrose consumption}} \times 100\%$$

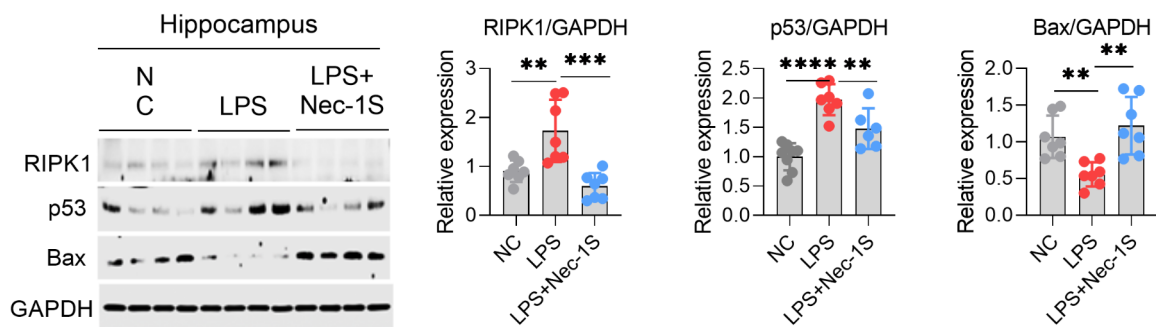
#### Forced swimming test (FST)

The forced swimming test (FST) was performed according to previously developed protocols [23]. The experimental animals were trained for swimming, and pre-experiment FST was performed to select healthy and normal mice. Animals were placed in a Plexiglas cylinder (height: 70 cm, diameter: 30 cm) filled with water over the 30 cm level at a temperature of  $23 \pm 1^\circ\text{C}$ , to perform the FST test. The video was taped for 6 min, and the last 5 min were blindly analyzed. Mice were considered immobile when they remained floating motionless in the water and just making a move to keep their nose above the water's surface. The horizontal movement

(A).



(B).



(C).

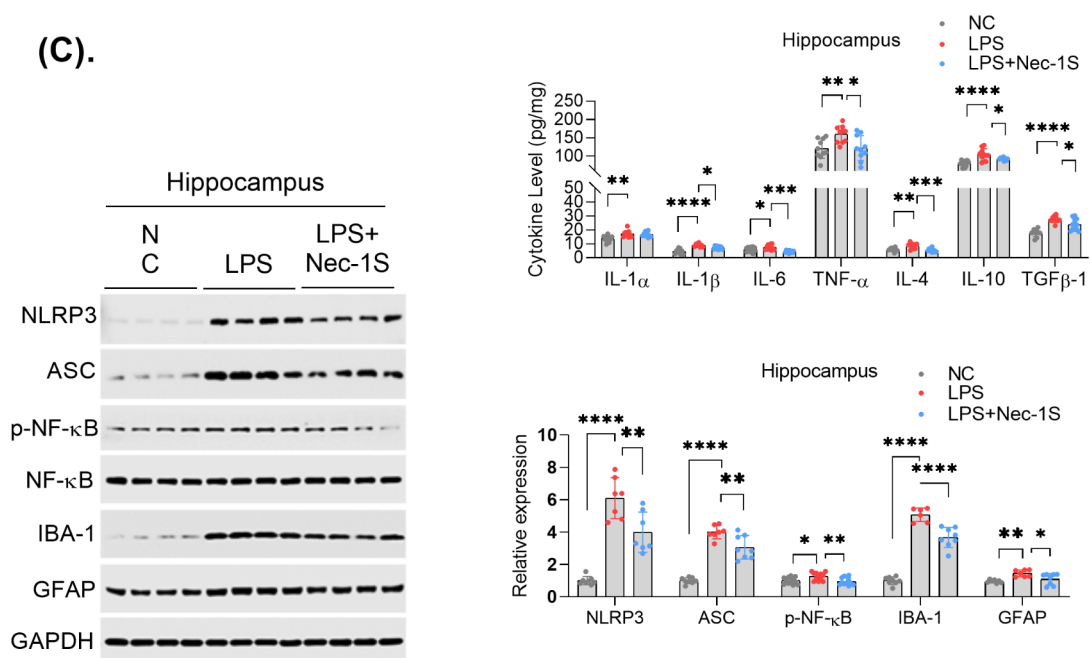


**Fig. 1** LPS activates RIPK1 in mice. (A) Drug treatment schedule and experimental approach (B) Immunoblots and Bar Graphs show expression of RIPK1, p53, and Bax in the hippocampal tissues ( $n=8$ ) (C) Representative immunoblots (left) and bar graphs show expression of NLRP3, ASC, NF-κB, IBA-1, and GFAP (right,  $n=8$ ), ELISA analysis shows the level of cytokines. All the values were normalized with loading control GAPDH ( $n=8-10$ ). All the values are expressed as mean  $\pm$  SEM, one-way ANOVA followed by Turkey's multiple comparison tests. \* $p < 0.05$ , \*\* $p < 0.01$ , \*\*\* $p < 0.001$ , \*\*\*\* $p < 0.0001$



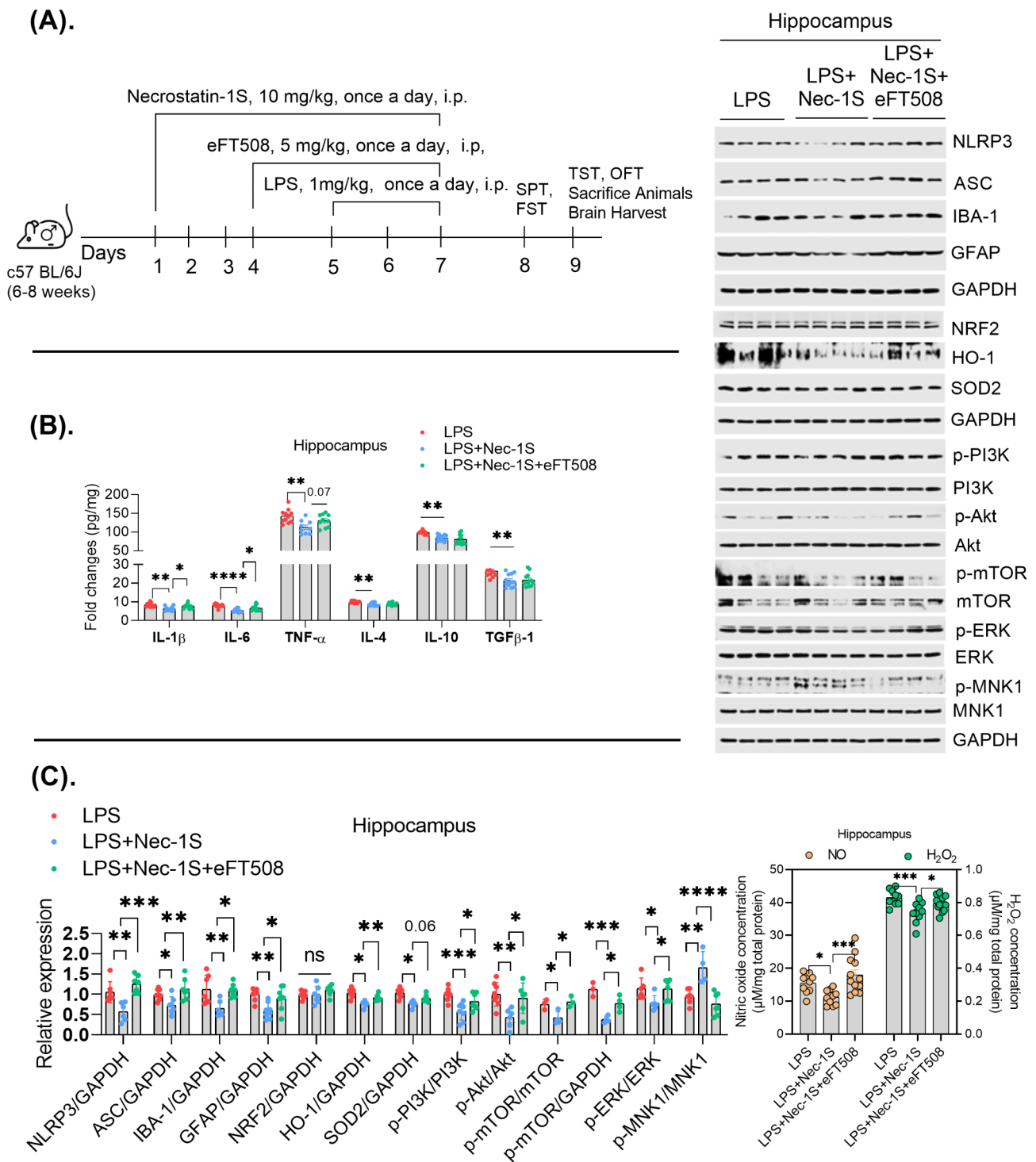


**Fig. 2** eFT508 treatment reversed the Nec-1 S effect in the presence of LPS. **(A)** Drug treatment schedule and experimental approach **(B)** Relative cytokine level ( $n=9-12$ ) **(C)** Representative immunoblots and bar graphs show expression of NLRP3, ASC, IBA-1, GFAP, NRF2, HO-1, SOD2, PI3K, Akt, mTOR, ERK, and MNK1, ( $n=6-8$ ). All the values were normalized with loading control GAPDH and are expressed as mean  $\pm$  SEM, one-way ANOVA followed by Turkey's multiple comparison tests. \* $p < 0.05$ , \*\* $p < 0.01$ , \*\*\* $p < 0.001$ , \*\*\*\* $p < 0.0001$

of the animals throughout the cylinder was defined as swimming, while vertical movement against the cylinder wall was defined as climbing. EthoVision XT was used to record the video and analysis.

#### **Tail suspension test (TST)**

The tail suspension test was performed as described previously [22, 24]. Briefly, the mice were individually suspended about 40 cm above the floor by their tail with the tape in the rectangular compartment (55 height × 20 widths × 11.5 cm depth). A total of 5 min of video were recorded and analyzed. EthoVision XT software was used to record and analyze the data.

#### **ELISA**

Frozen hippocampal tissue was lysed in RIPA buffer and homogenized on ice. Following centrifugation, supernatants were collected. Total protein concentration was determined using the BCA Protein Concentration Determination Kit (Beyotime, Shanghai, China). Samples were stored at freezing temperatures until further analysis.

Cytokine levels were quantified using ELISA kits (ABclonal, Wuhan, China) according to the manufacturer's protocol. Briefly, 100 µL of standard or sample diluent was added to each well of a 96-well plate and incubated for 2 h at 37 °C. Subsequent steps involved washing, incubation with biotin-conjugated antibody (1 h at 37 °C), washing, incubation with streptavidin-HRP (30 min at 37 °C), and final colourimetric detection at 450 nm. Cytokine concentrations were calculated based on the standard curve and normalized to total protein content.

#### **Nitric oxides(NO) and hydrogen peroxide (H<sub>2</sub>O<sub>2</sub>) measurement**

NO and H<sub>2</sub>O<sub>2</sub> were analyzed by commercially available kits (Beyotime, Shanghai, China) [25, 26]. Briefly, for the NO detection, 2 µL of the sample (serum/homogenates) were added to the mixture of Reagents (Gryess Reagent) R1+R2 (100 µL+100 µL), and absorbance was recorded at 540 nm. Similarly, for the H<sub>2</sub>O<sub>2</sub> detection, a 2 µL sample (serum/homogenates) was added to the 100 µL of the detection reagent, and after 30 min room temperature incubation, the absorbance was recorded at 560 nm.

#### **Cell viability**

Cell viability using cell counting kit-8 of MedChemExpress (Monmouth Junction, NJ, USA). Briefly, inoculate cell suspension (100 µL/well) in a 96-well plate. Add different concentration drugs (Nec-1 S/Citronellol) to the cell medium and pre-incubate the plate in a humidified incubator at 37 °C, 5% CO<sub>2</sub>. After the drug treatment time, add 10 µL of the CCK-8 solution to each well of the plate. Then, incubate the plate for 1–2 h in the incubator

and measure the absorbance at 450 nm using a microplate reader.

#### **BV2/N2a cell line culture protocol and stimulation**

Mouse microglial BV2 cell lines and neuroblastoma N2a cell lines were grown in high glucose Dulbecco's modified Eagle's medium (DMEM) supplemented with 10% fetal bovine serum (FBS) (Gibco, Waltham, MA). The cells were maintained in a humidified incubator with 95% air and a 5% CO<sub>2</sub> atmosphere at 37 °C. Medium containing the appropriate agents was replaced every other day. The drug was added to the cell medium when the cells grew to a density of about 90%.

In the first in vitro experiment, BV2 cells were treated with Nec-1 S at concentrations of 1 µM, 5 µM, 10 µM, or 20 µM for 8 h, followed by LPS (100 µM) for 4 h. However, subsequent experiments focused on treatments with 10 µM or 20 µM Nec-1 S (Fig. 3A).

In the second experiment, BV2 cells were treated with Citronellol (50 µg/mL) for 5 h, followed by eFT508 (1 µM) for 1 h before cell collection and further analysis (Fig. 4C).

In the third in vitro experiment, N2a cells were initially treated with Nec-1 S (10 µM) for 8 h, followed by LPS (100 ng/mL). Subsequently, the cells were treated with eFT508 (1 µM) for 1 h before final collection and analysis (Fig. 5A).

#### **Golgi staining**

The FD Rapid Golgi Stain Kit (FD Neuro Technologies, Ellicott City, MD) was used to perform Golgi staining. After removal, the animal brain was rinsed quickly in double distilled water, immersed in impregnation solutions (A/B) (5 ml solution for each tissue), and stored at room temperature for 2 weeks. The brain tissues were transferred to solution C and stored for 72 h (the solution was replaced after 24 h), followed by freezing. Afterwards, 100- to 200-µm sections were prepared using a sliding microtome and mounted to gelatine-coated microscope slides. Then the brain tissue was placed in a staining solution for 10 min, rinsed with double distilled water, followed by dehydration (sequential rinse 50%, 75%, and 95% ethanol) and xylene treatment, and finally, examined under an inverted fluorescence microscope IX73 Olympus.

#### **Western blotting**

According to the developed protocols, western blotting was performed. Briefly, Denatured samples (boiled at 100 °C for 10 min) were separated on SDS-PAGE and then transferred to the nitrocellulose membrane. The membrane was blocked with non-fat milk in TBST (Tris-buffered saline, 0.1% Tween 20), then incubated in primary antibody (1: 500; 1:1,000) overnight at 4 °C. The

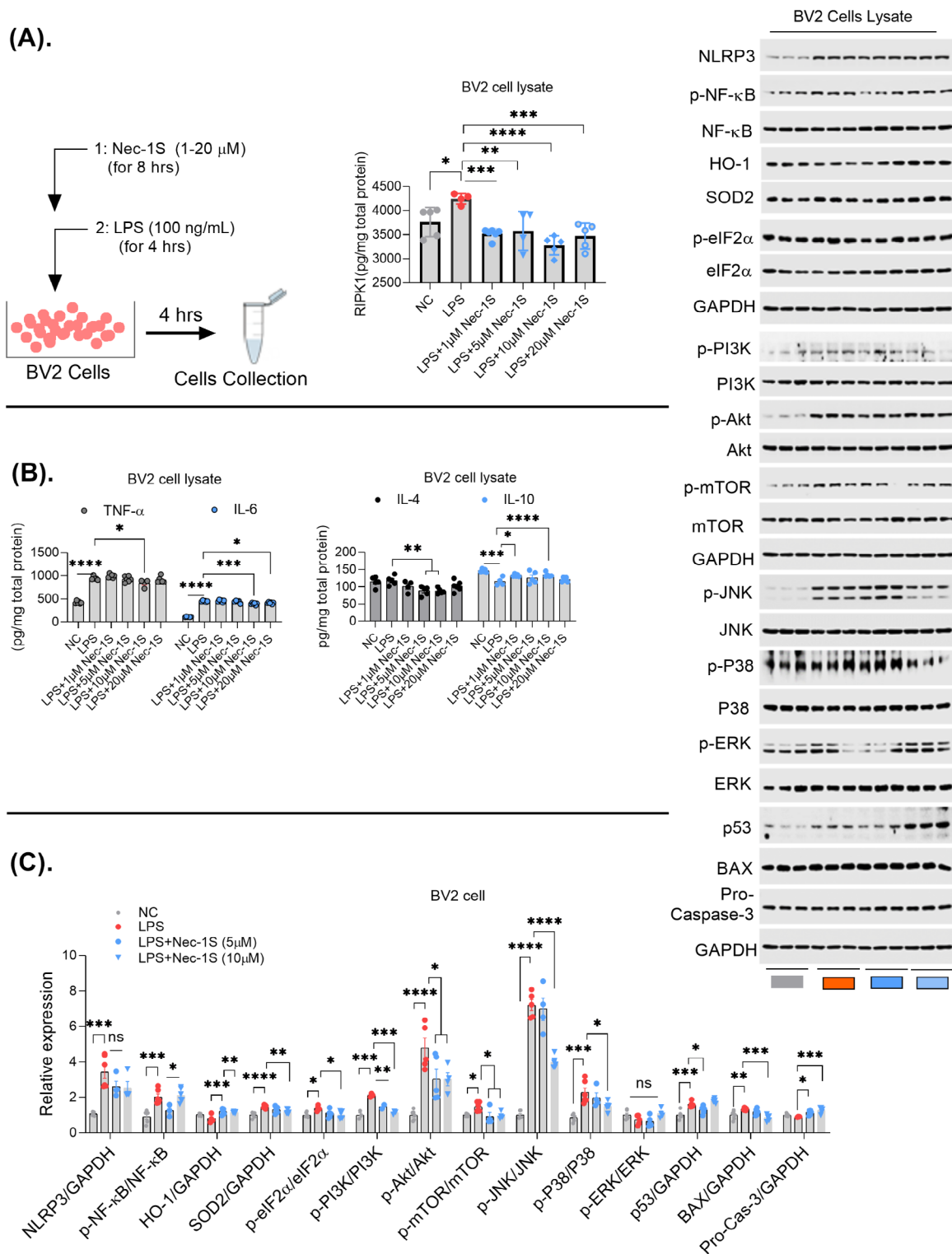
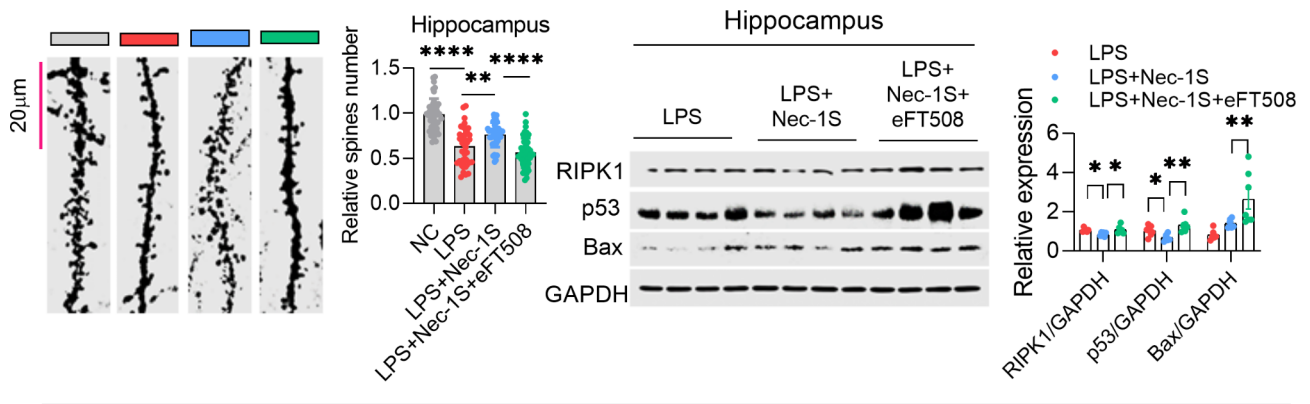
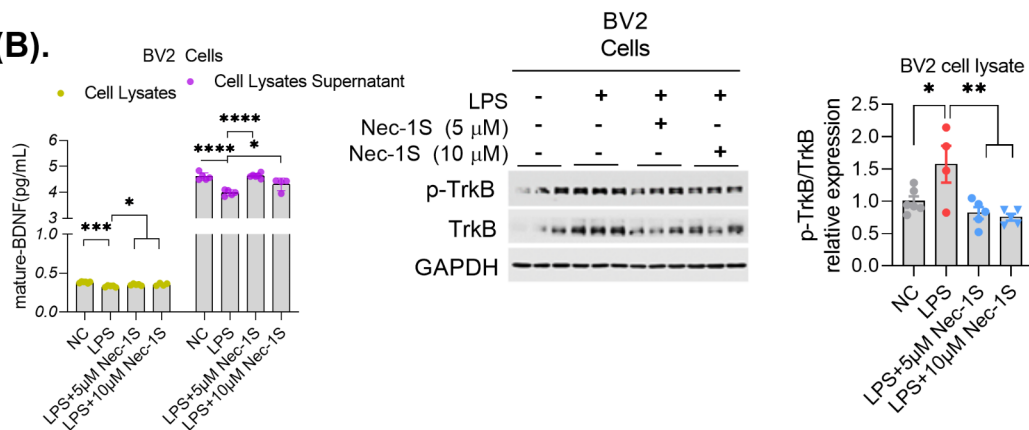


**Fig. 3** Nec-1 S treatment alleviates inflammation in BV2 cells. **(A)** BV2 cells treatment schedule and Bar graphs show an expression of RIPK1 expression ( $n=4-6$ ) **(B)** Representative quantitative graphs show the level of Cytokines in the BV2 Cells lysates ( $n=4-6$ ) **(C)** Representative western blot images showing NLRP3, NF- $\kappa$ B, HO-1, SOD2, p-eIF2 $\alpha$ , eIF2 $\alpha$ , PI3K, Akt, mTOR, p-JNK, JNK, p-P38, P38, p53, Bax, and Caspase3 expression ( $n=4-6$ ). All the values were normalized with loading control GAPDH. All values were expressed as mean  $\pm$  SEM, one-way ANOVA followed by post hoc analysis. \* $p < 0.05$ , \*\* $p < 0.01$ , \*\*\* $p < 0.001$ , \*\*\*\* $p < 0.0001$

(A).



(B).



(C).

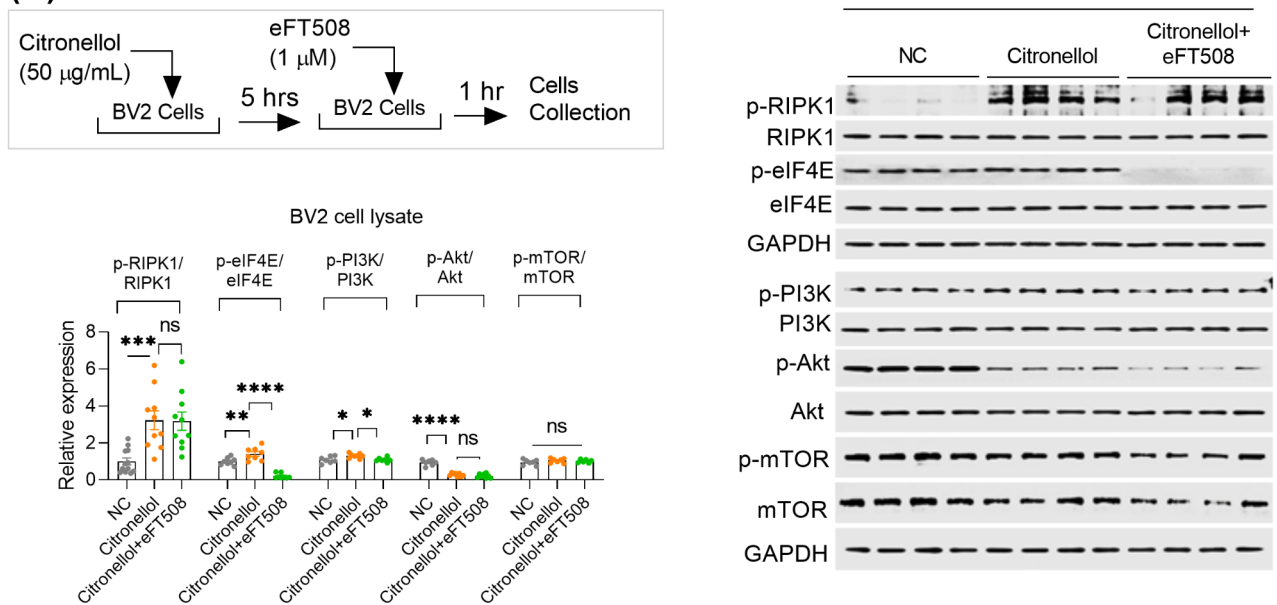


Fig. 4 (See legend on next page.)

(See figure on previous page.)

**Fig. 4** eFT508 treatment to BV2 cells in the presence of LPS. **(A)** eFT508 treatment reversed Nec-1 S effects on spine numbers and RIPK1 expression. Representative images of Golgi staining and bar graphs show spin numbers in the hippocampus of experimental subjects (right,  $n=4$ ). Immunoblots and bar graphs show the expression of RIPK1, p53, and Bax in the hippocampal tissue of the experimental mice (left,  $n=6-8$ ). **(B)** Quantitative bar graphs show mature-BDNF levels in the BV2 cells analyzed via ELISA (Left). Immunoblots and bar graphs show the expression of p-TrkB in the BV2 Cells ( $n=4-6$ ). **(C)** Citronellol and eFT508 treatment schedule. Bar graphs and immunoblots show expression/phosphorylation of RIPK1, eIF4E, PI3K, Akt, and mTOR ( $n=6-8$ ). All the values were normalized with loading control GAPDH and are expressed as mean  $\pm$  SEM, one-way ANOVA followed by Turkey's multiple comparison tests. \* $p < 0.05$ , \*\* $p < 0.01$ , \*\*\* $p < 0.001$ , \*\*\*\* $p < 0.0001$

next day, the membrane was treated with a secondary antibody (1:1,000) for 1 h at room temperature. The ECL Super signal chemiluminescence kit was used according to the manufacturer's protocol for detection. Blots were developed using Chemidoc mp Bio-rad. The densitometry analysis of the bands was performed using image lab software. Primary antibody information can be found in Table 1.

### Statistical analysis

Western blot bands and morphological data were analyzed using ImageJ and image lab software (Image J 1.30) and GraphPad Prism 8 software. Data were presented as mean  $\pm$  SEM. One-way ANOVA followed post-hoc Tukey Multiple Comparison tests to compare different groups.  $P < 0.05$  was regarded as significant. \*:  $p < 0.05$ , \*\*:  $p < 0.01$ , \*\*\*:  $p < 0.001$  and \*\*\*\*:  $p < 0.0001$ .

## Results

### RIPK1 inhibition averted LPS-induced neuroinflammation

LPS is a widely accepted neuroinflammatory agent [27]. To evaluate our hypothesis, mice were administered Nec-1 S for seven days, followed by LPS injection (intraperitoneally) for the final three days (Fig. 1A). We first validated RIPK1 inhibition in the hippocampus. LPS treatment significantly elevated RIPK1 expression, an effect reversed by Nec-1 S treatment. Furthermore, changes in the expression of p53 tumor suppressor (p53) and BCL2-Associated X (Bax), known downstream targets of RIPK1, corroborated the downregulation of RIPK1 (Fig. 1B).

To investigate RIPK1's role in neuroinflammation, we measured cytokines (IL-1 $\alpha$ , IL-1 $\beta$ , IL-6, TNF- $\alpha$ , IL-4, IL-10, TGF $\beta$ -1) and inflammatory markers in the hippocampus of experimental mice. Nec-1 S treatment significantly reduced LPS-induced increases in these cytokines and inflammatory proteins (NLRP3, ASC, p-NF- $\kappa$ B, IBA-1, GFAP) (Fig. 1C), supporting RIPK1's involvement in LPS-induced neuroinflammation. We also observed increased nuclear p-NF- $\kappa$ B in BV2 cells after LPS treatment, which was reversed by Nec-1 S (Fig. 6A).

To further explore the underlying mechanisms, we measured factors linked to neuroinflammation (NO, H<sub>2</sub>O<sub>2</sub>, NRF2/HO-1/SOD2, PI3K/Akt/mTOR, P38/ERK). Similar to NO and H<sub>2</sub>O<sub>2</sub>, Nec-1 S decreased these factors in the hippocampus of LPS-treated mice (Fig. 6B),

suggesting RIPK1's influence on inflammatory and oxidative pathways.

To validate these findings in vitro, we treated BV2 cells with Nec-1 S followed by LPS (Fig. 3A). Nec-1 S reduced proinflammatory cytokines (TNF- $\alpha$ , IL-6) but unexpectedly decreased IL-4, unlike IL-10 (Fig. 3B). Additionally, Nec-1 S inhibited Recombinant NLR Family, Pyrin Domain Containing Protein 3 (NLRP3), p-NF- $\kappa$ B, Heme Oxygenase 1(HO-1), Superoxide Dismutase 2(SOD2), Eukaryotic Translation Initiation Factor 2- $\alpha$ (eIF2 $\alpha$ ), PI3K/Akt/mTOR, JNK/P38/ERK, and Bax expression in LPS-treated BV2 cells (Fig. 3C). These results were replicated in N2a cells (Fig. S2).

Next, to investigate a potential interaction between RIPK1 and eIF4E in LPS-induced neuroinflammation, we treated mice with the MNK inhibitor eFT508 to concurrently inhibit MNK and eIF4E in the presence of LPS and Nec-1 S (Fig. 2A). MAP kinase signal-integrating kinase 1(MNK1) is a protein kinase that plays a crucial role in eukaryotic cells, and MNK1 is one of the key kinases responsible for phosphorylating eIF4E on serine 209 [28]. Surprisingly, eFT508 treatment significantly elevated cytokine levels (IL-1 $\beta$ , IL-6, TNF- $\alpha$ ) in the hippocampus of LPS-treated mice despite Nec-1 S administration (Fig. 2B). Consistent with this, we observed increased expression of NLRP3, ASC, IBA-1, GFAP, and HO-1, as well as enhanced phosphorylation of PI3K, Akt, mTOR, and ERK in the hippocampus of LPS-treated mice treated with both eFT508 and Nec-1 S. However, eFT508 reduced MNK1 phosphorylation in the hippocampus of LPS and Nec-1 S-treated mice. Notably, inhibiting eIF4E reversed the anti-inflammatory effects of Nec-1 S by increasing NO and H<sub>2</sub>O<sub>2</sub> levels (Fig. 2C). In addition, eFT508 treatment attenuated Nec-1 S effect by modulating IBA-1, GFAP and ASC/TMS1 expression in the hippocampus of the mice (Fig. S1). These findings strongly suggest a crucial role for RIPK1 and its interaction with eIF4E in mediating LPS-induced neuroinflammation.

### RIPK1 inhibition relieved LPS-induced depressive-like behaviors and improved synaptic defects via eIF4E signaling

A concurrent impairment of neuroinflammation to depressive-like behaviors is well-established from the documented research [29]. To assess the impact of RIPK1 inhibition on LPS-induced depressive-like behaviors and synaptic plasticity, we conducted behavioral tests and



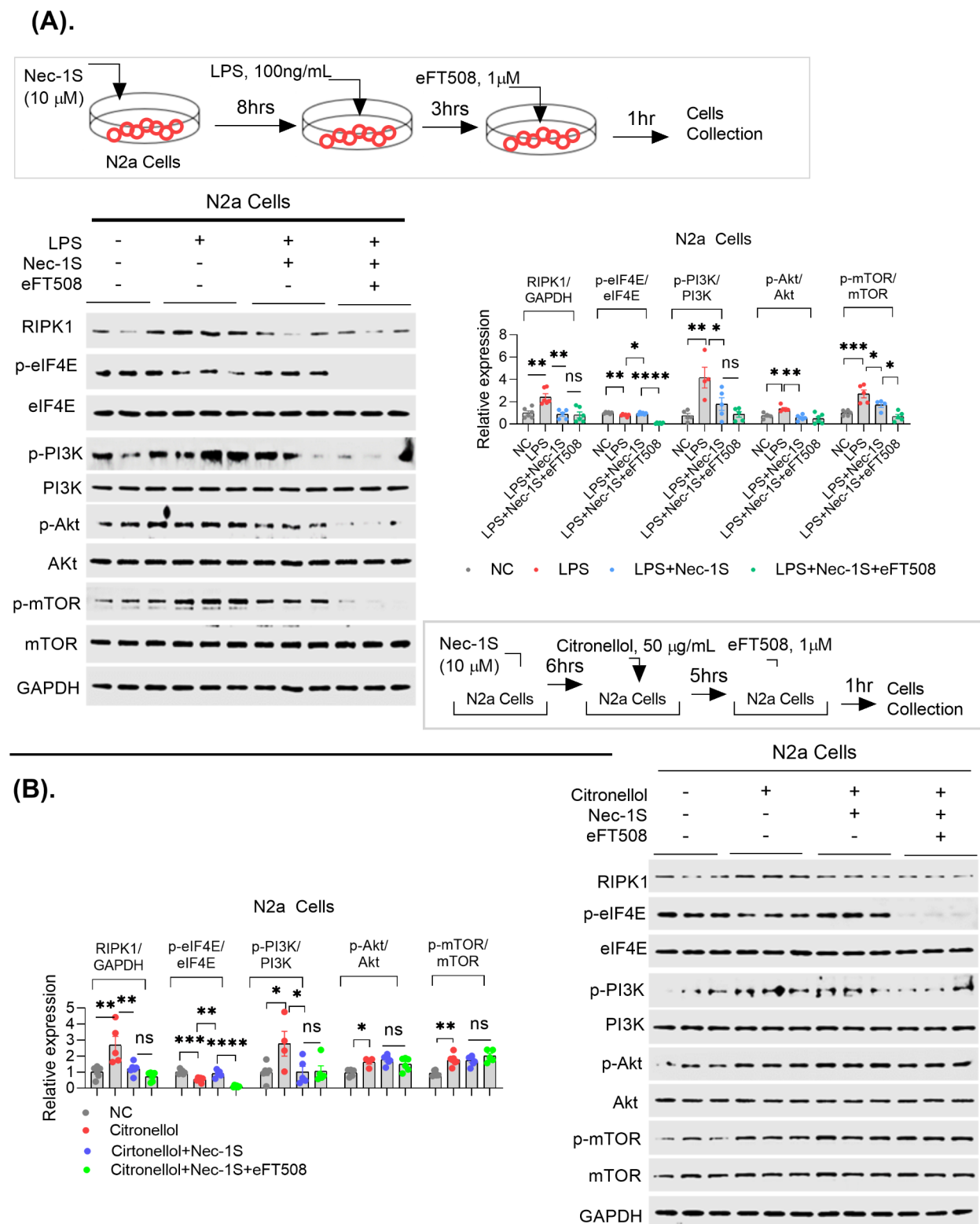


**Fig. 5** eFT508 modified citronellol effects in N2a Cells. **(A)** Drug (Nec-1 S and LPS) treatment schedule. Immunoblots (right) and bar graphs (left) show the expression and phosphorylation of RIPK1, eIF4E, PI3K, Akt, and mTOR in the N2a Cells ( $n=6-8$ ). **(B)** Drug treatment schedule (left), Quantitative Bar graphs, and immunoblots show expression/phosphorylation of RIPK1, eIF4E, PI3K, Akt, and mTOR ( $n=6-8$ ). All the values were normalized with loading control GAPDH and are expressed as mean $\pm$ SEM, one-way ANOVA followed by Turkey's multiple comparison tests. \* $p < 0.05$ , \*\* $p < 0.01$ , \*\*\* $p < 0.001$ , \*\*\*\* $p < 0.0001$



**Table 1** Detailed antibody information

Antibody	Company	Lot Number	Dilute	Source
NLRP3	Cell signaling technology	15,101	1/1000	Rabbit
ASC/TSM	Cell signaling technology	67,824	1/1000	Rabbit
p-NF-κB(Ser536)	Cell signaling technology	3033	1/1000	Rabbit
NF-κB	Cell signaling technology	8242	1/1000	Rabbit
Iba-1	Cell signaling technology	17,198 S	1/1000	Rabbit
GFAP	Cell signaling technology	3670 S	1/1000	Mouse
GAPDH	Cell signaling technology	5174	1/1000	Rabbit
IRE1α	Cell signaling technology	3294	1/1000	Rabbit
p-AMPKα(Thr172)	Cell signaling technology	2535	1/1000	Rabbit
AMPKα	Cell signaling technology	5832	1/1000	Rabbit
p-TrkB(Tyr705)	abcam	ab229908	1/1000	Rabbit
TrkB	Cell signaling technology	4603	1/1000	Rabbit
BDNF	abcam	ab108319	1/1000	Rabbit
p-eEF2(T56)	Cell signaling technology	2331	1/1000	Rabbit
eEF2	abcam	ab33523	1/1000	Rabbit
p-eIF2α(S51)	Cell signaling technology	3597	1/1000	Rabbit
eIF2α	Cell signaling technology	9722	1/1000	Rabbit
p-eIF4E(S209)	Cell signaling technology	9741	1/1000	Rabbit
eIF4E	Cell signaling technology	2067	1/1000	Rabbit
PSD95	abcam	ab18258	1/1000	Rabbit
SNAP25	abcam	ab41455	1/1000	Rabbit
Synapsin-1	Cell signaling technology	25,297	1/1000	Rabbit
Synaptophysin	Cell signaling technology	36,406	1/1000	Rabbit
Nrf2	Cell signaling technology	12,721	1/1000	Rabbit
HO-1	Cell signaling technology	70,081	1/1000	Rabbit
SOD2	Cell signaling technology	13,194	1/1000	Rabbit
p-PI3K(Tyr458/199)	Cell signaling technology	4228	1/1000	Rabbit
PI3K	Cell signaling technology	4257	1/1000	Rabbit
p-Akt(Ser473)	Cell signaling technology	4060	1/1000	Rabbit
Akt	Cell signaling technology	4691	1/1000	Rabbit
p-mTOR(Ser2448)	Cell signaling technology	2971	1/1000	Rabbit
mTOR	Cell signaling technology	2972	1/1000	Rabbit
p-p38(T180/Y182)	Cell signaling technology	4511	1/1000	Rabbit
p38	Cell signaling technology	9212	1/1000	Rabbit
p-JNK(Thr183/Tyr185)	Cell signaling technology	4668	1/1000	Rabbit
JNK	Cell signaling technology	9252	1/1000	Rabbit
p-ERK(T202/Y204)	Cell signaling technology	4370	1/1000	Rabbit
ERK	Cell signaling technology	4695	1/1000	Rabbit
GFAP	merck	3,140,011	1/400	Mouse
Iba-1	Wako	019-19741	1/400	Rabbit
p-RIPK1(Ser161)	Proteintech	66854-1-Ig	1/1000	Mouse
RIPK1	abcam	ab202985	1/1000	Rabbit
p53	Santa Cruz	sc-98	1/500	Mouse
Bax	Cell signaling technology	2772	1/1000	Rabbit
PERK	Cell signaling technology	3192	1/1000	Rabbit
Drp1	Cell signaling technology	8570	1/1000	Rabbit
Mfn1	Santa Cruz	sc-166,644	1/500	Mouse
OPA1	Cell signaling technology	80,471	1/1000	Rabbit
PGC1α	Abcam	ab54481	1/1000	Rabbit
Complex 2	Abcam	ab14714	1/1000	Mouse
Complex 3	Abcam	ab14746	1/1000	Mouse
Complex 5	Abcam	ab14748	1/1000	Mouse
p-MNK1(Thr197/202)	Cell signaling technology	2111	1/1000	Rabbit

**Table 1** (continued)

Antibody	Company	Lot Number	Dilute	Source
MNK1	Cell signaling technology	2195	1/1000	Rabbit
Caspase-3	Cell signaling technology	9662	1/1000	Rabbit

examined synaptic markers. Nec-1 S treatment attenuated LPS-induced depressive-like behaviors, as evidenced by decreased immobility and increased sucrose preference (Fig. 7A). Concurrently, Nec-1 S reversed LPS-mediated impairments in synaptic protein expression (mature-BDNF, p-TrkB, PSD95, SNAP25, Synaptophysin, Synapsin-1, and p-eIF4E) and spine density (Figs. 7B and 4A). However, eFT508 administration reversed these beneficial effects of Nec-1 S, except for PSD95 expression (Fig. 7C). Furthermore, eIF4E inhibition potentiated RIPK1, p53, and Bax expression in the LPS+Nec-1 S-treated mice hippocampus. Nec-1 S also rescued LPS-induced reductions in BDNF and p-TrkB expression in BV2 cells (Fig. 4B).

#### Interplay between RIPK1 and eIF4E

To further elucidate the intricate relationship among RIPK1, eIF4E, and PI3K, we investigated the influence of PI3K inhibition on this axis. Given the well-established interplay between RIPK1 and PI3K signaling in diverse cellular functions, we employed Wortmannin to inhibit PI3K in BV2 cells. Unexpectedly, Wortmannin treatment augmented BDNF expression. Conversely, it attenuated phosphorylation of RIPK1, eIF4E, PI3K, AKT, and mTOR, in LPS-stimulated BV2 cells (Fig. S3).

To further elucidate the underlying mechanisms, we investigated the interactions between RIPK1, eIF4E, and PI3K in the absence of LPS using citronellol and eFT508 treatment in BV2 cells (Fig. 4C). Citronellol decreased mature BDNF expression (Fig. S4, right) while concurrently increasing p-RIPK1, p-eIF4E, and p-PI3K levels. These effects were reversed by Nec-1 S treatment (Fig. S4, left). Moreover, eFT508 reduced the phosphorylation of eIF4E, PI3K, and AKT but had no significant impact on p-RIPK1 or p-mTOR (Fig. 4C). These findings collectively indicate a complex interplay among RIPK1, eIF4E, and PI3K signaling pathways.

Next, we extended our investigation to N2a cells to elaborate further on the mechanisms. Pre-treatment with Nec-1 S attenuated RIPK1 expression while concurrently increasing p-eIF4E and decreasing PI3K/Akt/mTOR phosphorylation. Subsequent eFT508 treatment reduced p-eIF4E and p-mTOR levels, with no significant changes observed in RIPK1, p-PI3K, or p-Akt expression (Fig. 5A). Additionally, Nec-1 S-induced eIF4E phosphorylation was reversed by eFT508 in the presence of citronellol, without affecting p-PI3K, p-Akt, or p-mTOR levels (Fig. 5B). These results in N2a cells support the

complex interplay between RIPK1, eIF4E, and the PI3K/Akt/mTOR pathway.

#### Discussion

The present study unveils a novel role for RIPK1 in the pathophysiology of depression. Depletion of RIPK1 attenuated depressive-like behaviors that co-occurred with neuroinflammation. We demonstrate that LPS-induced activation of RIPK1 is associated with neuroinflammation, depressive-like symptoms, and synaptic impairment. Critically, these effects were mitigated by RIPK1 antagonism. Mechanistic investigations revealed that eIF4E inhibition reversed the beneficial effects of Nec-1 S by augmenting cytokine production, astrogliosis, microgliosis, and inflammatory signaling, concomitantly with synaptic dysfunction and oxidative stress. These findings were corroborated in N2a cells, and the effects of Nec-1 were validated by citronellol treatment in BV2 and N2a cells.

Neuroinflammation involvement in depression is well-established and documented, where it affects metabolism, neuroplasticity, and neurogenesis concurrent with cytokines production and HPA-axis activation [30]. Oodless studies are going on to avert and limit neuroinflammation by targeting the neuroinflammation regulatory factors and processes to suppress neurological diseases, including depression. Apropos, RIPK1 is considered a possible target for limiting neuroinflammation because it can switch inflammatory response via NF- $\kappa$ B dependent, apoptosis via caspase-8 dependent, and necroptosis via MLKL (mixed lineage kinase domain-like protein) dependently [13, 15]. Moreover, RIPK1 can be activated during TLR4-mediated necroptosis [31, 32]: a necrotic cell death of neurons and glial cells in the CNS. Thus, targeting necroptosis could be a potential mechanism to avert and relieve neuroinflammatory diseases, as suggested by a previous study [33, 34]. The present study demonstrates that LPS treatment significantly upregulated RIPK1 expression, accompanied by neuroinflammation. Mechanistically, LPS-induced TNF- $\alpha$  production in N2a cells triggered RIPK1 signaling, corroborating RIPK1 activation following LPS administration in our model. Notably, RIPK1 inhibition using Nec-1 S attenuated cytokine release, reduced glial activation, and suppressed inflammatory signaling in LPS-treated mice, suggesting a critical role for RIPK1 in LPS-induced neuroinflammation.

Mounting evidence favors that neuroinflammation concurs with depressive-like behaviors [35]. As we and

(A).

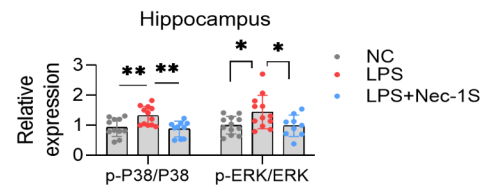
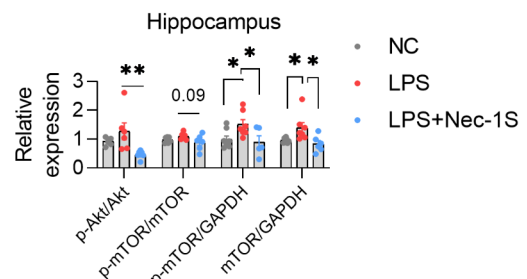
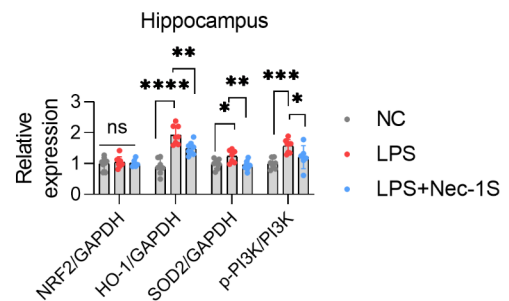
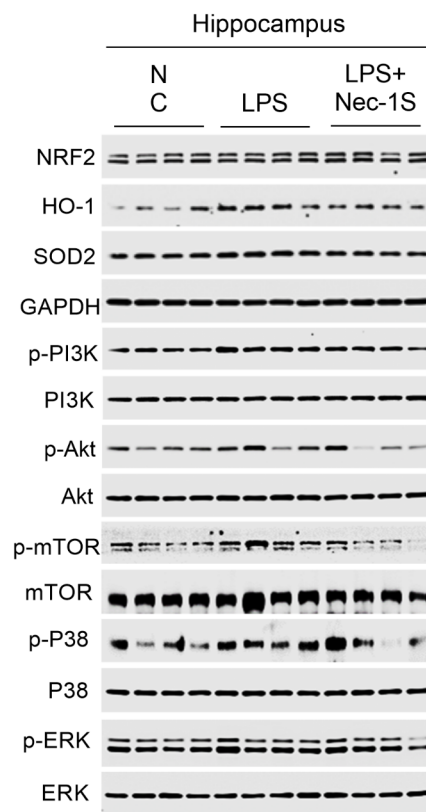
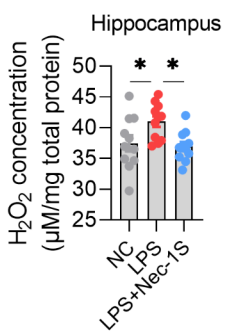
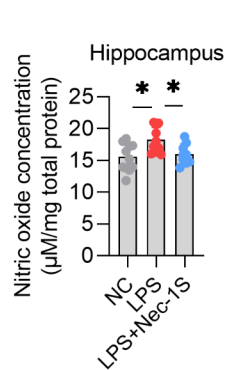
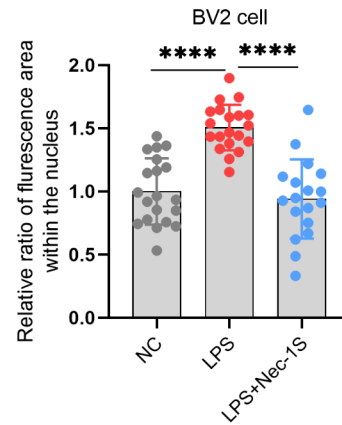
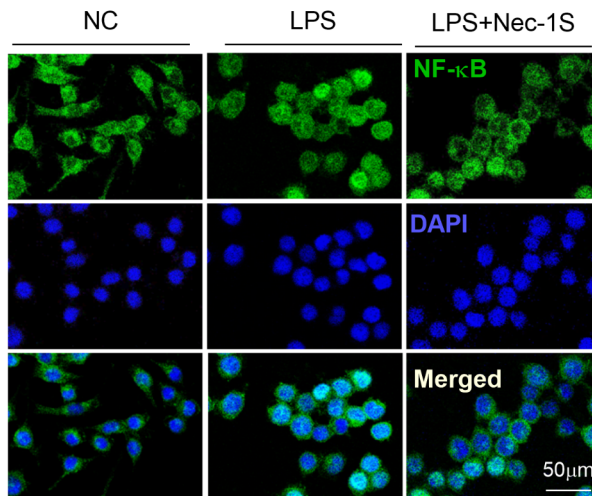
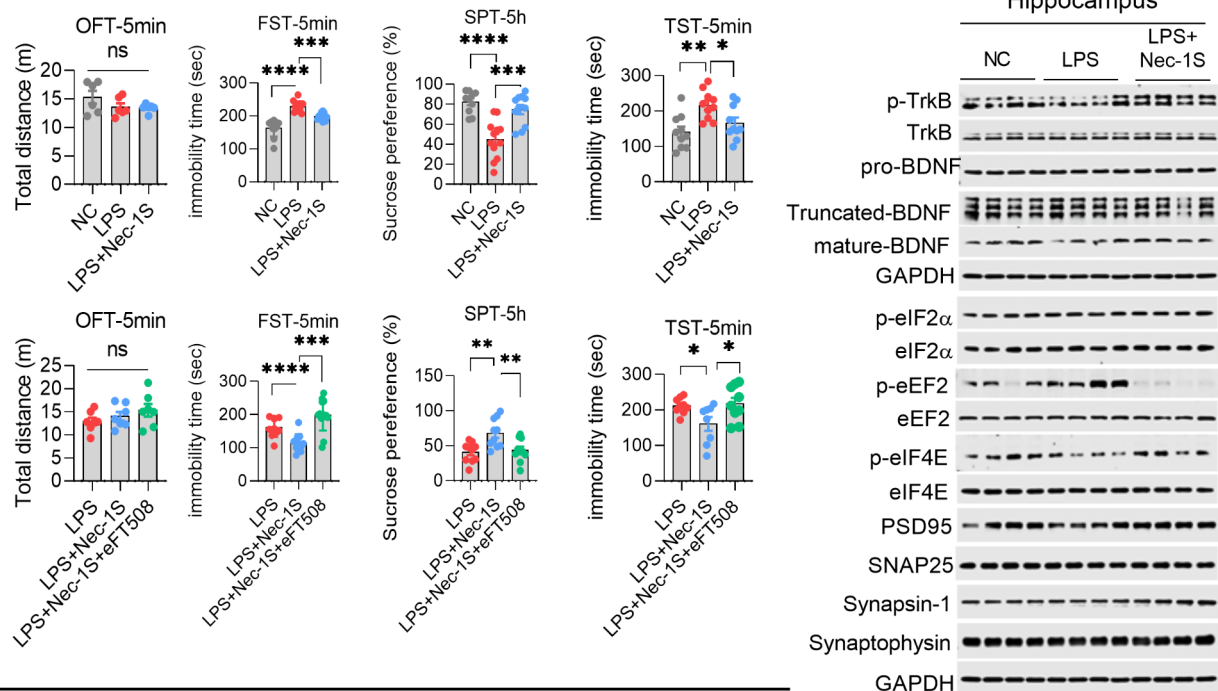
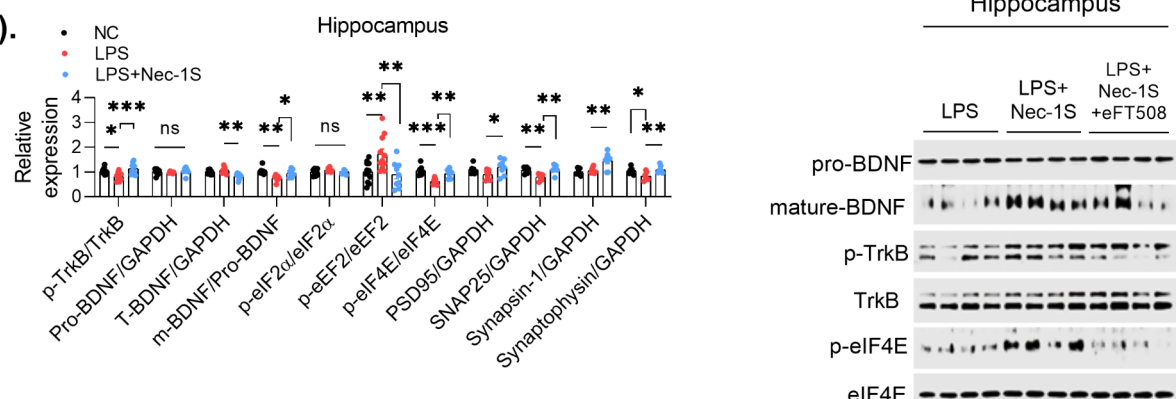


**Fig. 6** Nec-1 S treatment alleviates the inflammasome and redox signaling activation caused by LPS. **(A)** Immunofluorescence and Bar graphs show the expression of NF-κB in the nucleus of the BV2 cells. ( $n = 18-20$ ) **(B)** (left): Nitric oxide and hydrogen peroxide level in the hippocampal tissue of the experimental mice, (Right,  $n = 8-10$ ): Representative immunoblots and bar graphs showing relative expression/phosphorylation of NRF2, HO-1, SOD2, PI3K, Akt, mTOR, P38, JNK, and ERK expression ( $n = 6-8$ ). All the values were expressed as mean  $\pm$  SEM, one-way ANOVA followed by post hoc analysis. \* $p < 0.05$ , \*\* $p < 0.01$ , \*\*\* $p < 0.001$ , \*\*\*\* $p < 0.0001$

(A).



(B).



(C).

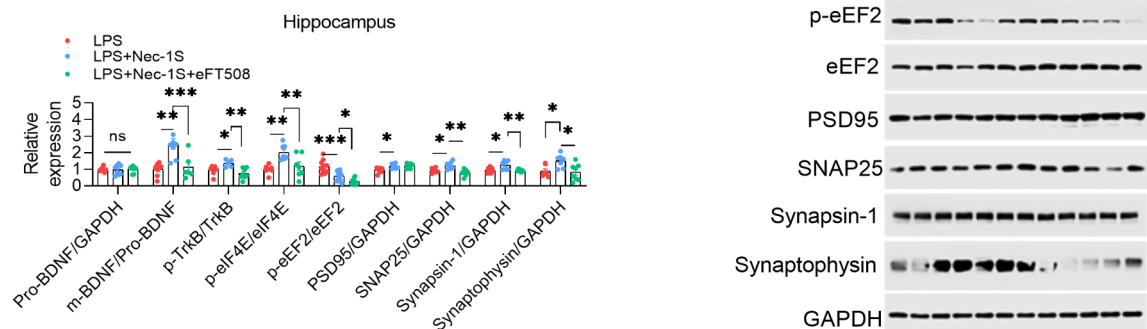


**Fig. 7** eFT508 treatment reversed the Nec-1 S antidepressant effect in the presence of LPS. **(A)** Representative bar graphs showing behavior tests, including OFT, FST, SPT, and TST. ( $n=10-12$ ) **(B)** Nec-1 S treatment improved LPS-altered expression of synaptic proteins, including TrkB, BDNF, eIF2 $\alpha$ , eIF4E, PSD95, SNAP25, Synapsin-1, and Synaptophysin ( $n=6-8$ ). **(C)** Bar graphs and Representative western blot images showing BDNF, TrkB, eIF4E, eEF2, PSD95, SNAP25, Synapsin-1, and Synaptophysin expression ( $n=6-8$ ). All the values were normalized with loading control GAPDH and are expressed as mean  $\pm$  SEM, one-way ANOVA followed by Turkey's multiple comparison tests. \* $p < 0.05$ , \*\* $p < 0.01$ , \*\*\* $p < 0.001$ , \*\*\*\* $p < 0.0001$

others reported previously, LPS-treated mice displayed enhanced cytokines levels and dysregulated inflammatory signaling coincident with altered synaptic signaling and reduced spine numbers [27, 29, 35]. It shows that LPS enhances peripheral cytokines level untimely transport to CNS, leading to glial cell activation. As the glial cells shape the synapse's structure, dysregulated glial cells in pathological conditions such as neuroinflammation could sculpt neuronal synapses by increasing or decreasing the elimination of synapses [36]. Our findings demonstrate that RIPK1 inhibition mitigated neuroinflammation and synaptic deficits, concomitantly ameliorating depressive-like behaviors. Nec-1 S treatment effectively reversed LPS-induced synaptic impairment in both the murine hippocampus and BV2 cells; the unexpected attenuation of RIPK1 inhibitor benefits by eFT508 treatment suggests a complex interplay between eIF4E and RIPK1 in the pathophysiology of neuroinflammation-associated synaptic dysfunction. eIF4E involves mRNA translation, and its (p-eIF4E) ablation downregulates I $\kappa$ B $\alpha$ , ultimately activating the transcription factor NF- $\kappa$ B, leading to cytokine production [37]. Surprisingly, in our findings, eIF4E inhibition by eFT508 reversed Nec-1 S effects by increasing neuroinflammation, inflammatory signaling dysregulation, and synaptic impairment. It proposes that RIPK1 contributes to neuroinflammation and synaptic impairments via dysregulating eIF4E signaling. Besides, recent studies have revealed a potential role of eIF4E in the antidepressant action of psychiatry drugs, including antidepressants [38].

Moreover, MNK1/2 phosphorylates eIF4E via MAPK/ERK signaling [39, 40], which we found also downregulated after eFT508 treatment, although it was increased after RIPK1 inhibition by Nec-1 S in LPS-treated mice hippocampus. It shows an interplay between RIPK1 and MNK1/2 in the regulation of eIF4E. Besides, active PI3K/mTORc1 signaling can increase eIF4E availability for translational initiation via downstream phosphorylation of 4E-BPs [41, 42]. Our study found decreased p-RIPK1, p-eIF4E, and p-PI3K/Akt/mTOR expression in the BV2 cells, further validating PI3K/Akt/mTOR signaling association with eIF4E via RIPK1. The RIPK1 agonist (Citronellol) enhanced p-eIF4E and p-PI3K expression, showing that RIPK1 could regulate eIF4E activity.

Previous studies have shown that RIPK1 activated the p-AKT/eIF4E signaling pathway during necroptosis and cell death via AKT, mTORC1, 4E-BP, and eIF4E pathway [18, 43]. It shows that RIPK1 contributes to different cell signaling via distinct mechanisms. As here from our findings, we may also propose that eIF4E acts downstream of RIPK1 because, in BV2 cells, RIPK1 activation enhances eIF4E activities by increasing its phosphorylation sequentially; it promotes cytokine production and reduces mature-BDNF release. Meanwhile, in the neuron, RIPK1

activation decreases eIF4E phosphorylation, which could affect synaptic protein production and, hence, neuroplasticity. Thus, during neuroinflammation, BV2 cells (microglia) promote high cytokine production and fewer BDNF releases, affecting synaptic signaling and synapses that could be linked to depressive-like behaviors.

In conclusion, RIPK1 contributes to LPS-induced neuroinflammation and depression. Moreover, eIF4E, recently linked to depression and neuroinflammation, was down-phosphorylated after RIPK1 inhibition, concurrent with the improved synaptic protein expression. Thus, RIPK1 is a potential target for neuroinflammation-coinciding depression via eIF4E signaling.

#### Abbreviations

AKT	Serine-threonine protein kinase
ANOVA	Analysis of variance
ASC/TSM1	Apoptosis-associated speck-like protein containing a CARD, PYD and CARD domain-containing protein
AMPK $\alpha$	5'-AMP-activated protein kinase subunit $\alpha$
BDNF	Brain-derived neurotrophic factors
Citronellol	2,6-DIMETHYL-2-OCTEN-8-OL
CNS	Central nervous system
eEF2	Eukaryotic elongation factor 2
eIF2 $\alpha$	Eukaryotic translation initiation factor 2 $\alpha$
eIF4E	Eukaryotic translation initiation factor 4E
ERK	Signal-regulated kinase
ELISA	enzyme-linked immunosorbent assay
eFT508	6'-[[6-Amino-4-pyrimidinyl]amino]-8'-methylspiro[cyclohexane-1,3'(2'H)-imidazo[1,5-A]pyridine]-1,5'-diketone
FST	Force swimming test
GFAP	Glial Fibrillary Acidic Protein
GAPDH	Glyceraldehyde-3-phosphate dehydrogenase
HO-1	Heme oxygenase 1
IL-1 $\alpha$	Interleukin 1 alpha
IL-1 $\beta$	Interleukin 1 beta
IL-6	Interleukin 6
IL-4	Interleukin 4
IL-10	Interleukin 10
IRE1 $\alpha$	Serine/threonine-protein kinase/endoribonuclease subunit $\alpha$
IBA1	Allograft inflammatory factor 1
JNK	stress-activated protein kinase
LPS	Lipopolysaccharides
mTOR	mammalian target of rapamycin
MAPK	Mitogen-Activated Protein Kinase
MDD	Major depressive disorder
Nec-1S	5-((7-Cl-1 H-indol-3-yl)Methyl)-3-Methylimidazolidine-2,4-dione)
Wortmannin	3 H-Furo[4,3,2-de]indeno[4,5-h]-2-benzopyran-3,6,9-trione,11-(acetyloxy)-1,6b,7,8,9a,10,11,11b-octahydro-1-(methoxymethyl)-9a,11b-dimethyl-(1 S,6bR,9aS,11R,11bR)
NLRP3	NLR family pyrin domain containing 3
NF- $\kappa$ B	Nuclear Factor Kappa B Subunit
NRF2	Nuclear factor erythroid 2-related factor 2
OFT	Open field test
PI3K	phosphatidylinositol 3-kinase
p38	Mitogen-activated protein kinase
PSD-95	postsynaptic density protein 95
RIPK1	receptor (TNFRSF)-interacting serine-threonine kinase 1
SPT	Sucrose preference test
SOD2	Superoxide dismutase [Mn], mitochondrial
SNAP25	Synaptosome Associated Protein 25
TST	Tail suspension test
TNF- $\alpha$	Tumor Necrosis Factor-alpha
TGF- $\beta$ 1	Transforming Growth Factor beta-1
TrkB	Tropomyosin receptor kinase B



## Supplementary Information

The online version contains supplementary material available at <https://doi.org/10.1186/s12964-024-01796-3>.

Supplementary Material 1

Supplementary Material 2

Supplementary Material 3

## Acknowledgements

Acknowledgements: Shenzhen-Hong Kong Institute of Brain Science-Shenzhen Fundamental Research Institutions (2022SHIBS0004) .

## Author contributions

Author contributions: Conceptualization: QG, TA, SL; Methodology: YH, RG, SM, CY, AL, YL, and QG; Investigation and Analysis: QG, TL, LH, and TA; Writing: TA, SL; Supervision: LH, XY, and SL. All authors read and approved the final manuscript.

## Funding

His work was supported by the National Natural Science Foundation of CHINA (NSFC GRANT NO. 82072112); Shenzhen-Hong Kong Institute of Brain Science No: GRANT NO: 2022SHIBS0004; Shenzhen Science and Technology Program GRANT NO: JCYJ20220530165207016, Cultivate fund of the second hospital of Shandong university GRANT NO:2022YP86, Clinical research fund of Shandong provincial medical association-special support of Qilu, GRANT NO YXH2022ZX02150)

## Data availability

No datasets were generated or analysed during the current study.

## Declarations

### Ethical approval and consent to participate

All experimental procedures were carried out according to the protocols approved by the Institutional Animal Care and Use Committee of Peking University Shenzhen Graduate School.

### Consent for publication

Not applicable.

### Competing interests

The authors declare no competing interests.

### Author details

<sup>1</sup>State Key Laboratory of Chemical Oncogenomics, School of Chemical Biology and Biotechnology, Peking University Shenzhen Graduate School, Shenzhen 518055, China

<sup>2</sup>College of Forensic Medicine, Institute of Forensic Injury, Xi'an Jiaotong University Health Science Center, Xi'an, Shanxi, China

<sup>3</sup>Hospital of Chengdu University of Traditional Chinese Medicine, No.39 Shi-er-Qiao Road, Chengdu, P.R. China

<sup>4</sup>Department of Neonatology, Affiliated Longhua People's Hospital, Southern Medical University (Longhua People's Hospital), Shenzhen 518190, China

<sup>5</sup>Cancer Center, The Second Hospital, Cheeloo College of Medicine, Shandong University, Jinan 250033, People's Republic of China

<sup>6</sup>Department of Psychiatry, University of Toronto, Toronto, ON, Canada

Received: 5 June 2024 / Accepted: 18 August 2024

Published online: 02 September 2024

## References

- Li W, Ali T, Zheng C, He K, Liu Z, Shah FA, Li N, Yu ZJ, Li S. Anti-depressive-like behaviors of APN KO mice involve Trkb/BDNF signaling related neuroinflammatory changes. *Mol Psychiatry*. 2022;27:1047–58.
- Schechter LE. Major depressive disorder. *Curr Pharm Des*. 2005;11:143–4.
- aan het Rot M, Mathew SJ, Charney DS. Neurobiological mechanisms in major depressive disorder. *CMAJ*. 2009;180:305–13.
- Drevets WC. Neuroimaging and neuropathological studies of depression: implications for the cognitive-emotional features of mood disorders. *Curr Opin Neurobiol*. 2001;11:240–9.
- Rădulescu I, Drăgoi AM, Trifu SC, Cristea MB. Neuroplasticity and depression: rewiring the brain's networks through pharmacological therapy (review). *Exp Ther Med*. 2021;22:1131.
- Bakunina N, Pariante CM, Zunszain PA. Immune mechanisms linked to depression via oxidative stress and neuroprogression. *Immunology*. 2015;144:365–73.
- Miller AH, Raison CL. The role of inflammation in depression: from evolutionary imperative to modern treatment target. *Nat Rev Immunol*. 2016;16:22–34.
- Pandey GN, Rizavi HS, Bhaumik R, Ren X. Innate immunity in the postmortem brain of depressed and suicide subjects: role of toll-like receptors. *Brain Behav Immun*. 2019;75:101–11.
- Raedler TJ. Inflammatory mechanisms in major depressive disorder. *Curr Opin Psychiatry*. 2011;24:519–25.
- Virtuoso A, De Luca C, Korai SA, Papa M, Cirillo G. Neuroinflammation and glial activation in the central nervous system: a metabolic perspective. *Neural Regen Res*. 2023;18:1025–6.
- Bajpai A, Verma AK, Srivastava M, Srivastava R. Oxidative stress and major depression. *J Clin Diagn Res*. 2014;8:Cc04–07.
- Meng H, Liu Z, Li X, Wang H, Jin T, Wu G, Shan B, Christofferson DE, Qi C, Yu Q, et al. Death-domain dimerization-mediated activation of RIPK1 controls necroptosis and RIPK1-dependent apoptosis. *Proc Natl Acad Sci U S A*. 2018;115:E2001–9.
- Mifflin L, Ofengeim D, Yuan J. Receptor-interacting protein kinase 1 (RIPK1) as a therapeutic target. *Nat Rev Drug Discov*. 2020;19:553–71.
- Yuan J, Amin P, Ofengeim D. Necroptosis and RIPK1-mediated neuroinflammation in CNS diseases. *Nat Rev Neurosci*. 2019;20:19–33.
- Zelic M, Pontarelli F, Woodworth L, Zhu C, Mahan A, Ren Y, LaMorte M, Gruber R, Keane A, Loring P, et al. RIPK1 activation mediates neuroinflammation and disease progression in multiple sclerosis. *Cell Rep*. 2021;35:109112.
- Chu E, Mychasiuk R, Hibbs ML, Semple BD. Dysregulated phosphoinositide 3-kinase signaling in microglia: shaping chronic neuroinflammation. *J Neuroinflamm*. 2021;18:276.
- He Y, Sun MM, Zhang GG, Yang J, Chen KS, Xu WW, Li B. Targeting PI3K/Akt signal transduction for cancer therapy. *Signal Transduct Target Ther*. 2021;6:425.
- Li F, Sun H, Yu Y, Che N, Han J, Cheng R, Zhao N, Guo Y, Huang C, Zhang D. RIPK1-dependent necroptosis promotes vasculature mimicry formation via eIF4E in triple-negative breast cancer. *Cell Death Dis*. 2023;14:335.
- Bhat M, Robichaud N, Hulea L, Sonenberg N, Pelletier J, Topisirovic I. Targeting the translation machinery in cancer. *Nat Rev Drug Discov*. 2015;14:261–78.
- Waterhouse EG, Xu B. New insights into the role of brain-derived neurotrophic factor in synaptic plasticity. *Mol Cell Neurosci*. 2009;42:81–9.
- Amorim IS, Lach G, Gkogkas CG. The role of the eukaryotic translation initiation factor 4E (eIF4E) in Neuropsychiatric disorders. *Front Genet*. 2018;9:561.
- Zhao X, Cao F, Liu Q, Li X, Xu G, Liu G, Zhang Y, Yang X, Yi S, Xu F, et al. Behavioral, inflammatory and neurochemical disturbances in LPS and UCMS-induced mouse models of depression. *Behav Brain Res*. 2019;364:494–502.
- Sekio M, Seki K. Lipopolysaccharide-induced depressive-like behavior is associated with  $\alpha$ 1-adrenoceptor dependent downregulation of the membrane GluR1 subunit in the mouse medial prefrontal cortex and ventral tegmental area. *Int J Neuropsychopharmacol* 2015, 18.
- Steru L, Chermat R, Thierry B, Simon P. The tail suspension test: a new method for screening antidepressants in mice. *Psychopharmacology*. 1985;85:367–70.
- Dai X, Sun Y, Jiang Z. Protective effects of vitamin E against oxidative damage induced by A $\beta$ 1–40Cu(II) complexes. *Acta Biochim Biophys Sin (Shanghai)*. 2007;39:123–30.
- Li YH, Yan ZQ, Jensen JS, Tullus K, Brauner A. Activation of nuclear factor kappaB and induction of inducible nitric oxide synthase by Ureaplasma urealyticum in macrophages. *Infect Immun*. 2000;68:7087–93.
- Li W, Ali T, He K, Liu Z, Shah FA, Ren Q, Liu Y, Jiang A, Li S. Ibrutinib alleviates LPS-induced neuroinflammation and synaptic defects in a mouse model of depression. *Brain Behav Immun*. 2021;92:10–24.
- Pyronnet S. Phosphorylation of the cap-binding protein eIF4E by the MAPK-activated protein kinase Mnk1. *Biochem Pharmacol*. 2000;60:1237–43.
- Ali T, Rahman SU, Hao Q, Li W, Liu Z, Ali Shah F, Murtaza I, Zhang Z, Yang X, Liu G, Li S. Melatonin prevents neuroinflammation and relieves depression by



- attenuating autophagy impairment through FOXO3a regulation. *J Pineal Res.* 2020;69:e12667.
30. Jeon SW, Kim YK. The role of neuroinflammation and neurovascular dysfunction in major depressive disorder. *J Inflamm Res.* 2018;11:179–92.
  31. Moriwaki K, Chan FK-M. Necroptosis-independent signaling by the RIP kinases in inflammation. *Cell Mol Life Sci.* 2016;73:2325–34.
  32. Dhuriya YK, Sharma D. Necroptosis: a regulated inflammatory mode of cell death. *J Neuroinflamm.* 2018;15:199.
  33. Yan ZY, Jiao HY, Chen JB, Zhang KW, Wang XH, Jiang YM, Liu YY, Xue Z, Ma QY, Li XJ, Chen JX. Antidepressant mechanism of traditional Chinese Medicine Formula Xiaoyaosan in CUMS-Induced Depressed Mouse Model via RIPK1-RIPK3-MLKL Mediated Necroptosis Based on Network Pharmacology Analysis. *Front Pharmacol.* 2021;12:773562.
  34. Zeb S, Ye H, Liu Y, Du H-P, Guo Y, Zhu Y-M, Ni Y, Zhang H-L, Xu Y. Necroptotic kinases are involved in the reduction of depression-induced astrocytes and fluoxetine's inhibitory effects on necroptotic kinases. *Front Pharmacol* 2023, 13.
  35. Zhao J, Bi W, Xiao S, Lan X, Cheng X, Zhang J, Lu D, Wei W, Wang Y, Li H, et al. Neuroinflammation induced by lipopolysaccharide causes cognitive impairment in mice. *Sci Rep.* 2019;9:5790.
  36. Lee E, Chung WS. Glial Control of Synapse Number in Healthy and diseased brain. *Front Cell Neurosci.* 2019;13:42.
  37. Herdy B, Jaramillo M, Svitkin YV, Rosenfeld AB, Kobayashi M, Walsh D, Alain T, Sean P, Robichaud N, Topisirovic I, et al. Translational control of the activation of transcription factor NF- $\kappa$ B and production of type I interferon by phosphorylation of the translation factor eIF4E. *Nat Immunol.* 2012;13:543–50.
  38. Amorim IS, Kedia S, Kouloulia S, Simbriger K, Gantois I, Jafarnejad SM, Li Y, Kampaite A, Pooters T, Romanò N, Gkogkas CG. Loss of eIF4E phosphorylation engenders Depression-like behaviors via Selective mRNA translation. *J Neurosci.* 2018;38:2118–33.
  39. Mody PH, Dos Santos NL, Barron LR, Price TJ, Burton MD. eIF4E phosphorylation modulates pain and neuroinflammation in the aged. *Geroscience.* 2020;42:1663–74.
  40. Joshi S, Plataniias LC. Mnk kinase pathway: Cellular functions and biological outcomes. *World J Biol Chem.* 2014;5:321–33.
  41. Richter JD, Sonenberg N. Regulation of cap-dependent translation by eIF4E inhibitory proteins. *Nature.* 2005;433:477–80.
  42. Haghghat A, Mader S, Pause A, Sonenberg N. Repression of cap-dependent translation by 4E-binding protein 1: competition with p220 for binding to eukaryotic initiation factor-4E. *EMBO J.* 1995;14:5701–9.
  43. Muendlein HI, Sarhan J, Liu BC, Connolly WM, Schworer SA, Smirnova I, Tang AY, Ilyukha V, Pietruska J, Tahmasebi S, et al. Constitutive Interferon attenuates RIPK1/3-Mediated cytokine translation. *Cell Rep.* 2020;30:699–e713694.

### Publisher's note

Springer Nature remains neutral with regard to jurisdictional claims in published maps and institutional affiliations.